EXPLORING STRENGTHENING MECHANISMS OF ULTRAFINE-GRAINED $Fe_{35}Mn_{27}Ni_{28}Co_5Cr_5$ HIGH-ENTROPY ALLOY PROCESSED BY SEVERE COLD ROLLING PROCESS

Majid Naseri, Ahmad Ostovari Moghaddam, Sergey Lezhnev, Nataliya Shaburova, Anatoliy Pellenen, Evgenii Bodrov, Evgeniy Panin, Marina Samodurova, Evgeny Trofimov

South Ural State University, 76 Lenin Ave.
Chelyabinsk 454080, Russia
E-mail: naserim@susu.ru, trofimovea@susu.ru

Received: 06 December 2023
Accepted: 26 January 2024
DOI: 10.59957/jctm.v59.i3.2024.20

ABSTRACT

This study describes the strengthening mechanisms of an ultrafine-grained (UFG) $Fe_{35}Mn_{27}Ni_{28}Co_5Cr_5$ high-entropy alloy (HEA) processed by severe cold rolling (SCR) process at room temperature. Microstructural evaluations were performed by field emission scanning electron microscopy (SEM) and transmission electron microscopy (TEM). The findings demonstrated that the development of deformation microstructures consisted of a single face-centered cubic (FCC) phase with stretched grains along the rolling direction and lamellar deformation bands after a 90 % reduction in thickness. Using the Nix-Gao model, the dislocation density was determined by measuring the microhardness indentation size effect. The results indicated that an increase in rolling deformation leads to an increase in dislocation density. The dislocation density increased from 2.28 $\times 10^9$ cm^{-2} for as-homogenized specimen to 8.65 $\times 10^9$ cm^{-2} after 90 % reduction in thickness. The yield strength of the UFG $Fe_{35}Mn_{27}Ni_{28}Co_5Cr_5$ HEA was 5.2 times (1155 MPa) higher than that of the as-homogenized state (225 MPa). Finally, an assessment was conducted on the relative contributions of individual mechanisms, such as dislocation and grain refinement, to the strengthening of the $Fe_{35}Mn_{27}Ni_{28}Co_5Cr_5$ HEA.

Keywords: high-entropy alloy, severe plastic deformation, ultrafine lamellar microstructures, strengthening mechanisms.

INTRODUCTION

High-entropy alloys (HEA) are a novel class of materials that contain five or more principal elements in equiatomic or nearly-equiatomic proportion, in contrast to traditional crystalline alloys that are typically based on one principal elements [1, 2]. This kind of alloy has drawn attention from scientists and engineers because of its innovative idea. Numerous elemental combinations can be used to effectively design HEAs with the necessary mechanical properties (such as high specific strength and good ductility, potential low- and/or high-temperature properties, good wear and fatigue resistance, and exceptional fracture toughness) [3 - 5]. It is anticipated that in the near future, cost-effective HEAs will be produced for use in a variety of industries. Among various HEA systems, FeMnNiCoCr HEA with a single FCC structure is one of the most widely investigated alloys owing to its superior properties [6, 7]. However, the relatively low strength (< 500 MPa) in the homogenized condition at room temperature limits its applications as a practical structural material.

Research efforts have tended to be application-driven and focused on developing strengthening techniques with promising mechanical properties, since high strength and ductility are critical for structural materials. The strategies of phase-transformation strengthening, precipitation hardening, and grain refinement strengthening were applied to achieve high mechanical performances in HEAs [8 - 11]. Furthermore,

another major research direction to elaborate on the potential applications of HEAs is using severe plastic deformation (SPD) processes such as high-pressure torsion (HPT), equal channel angular pressing (ECAP), and severe cold rolling (SCR) to tune the microstructure and mechanical properties of HEAs [12 - 15]. For instance, a bulk CoCrFeMnNi HEA with a grain size ranging from coarse to ultrafine grain was processed by cold rolling and annealing [16]. This resulted in an ultrafine-grained (UFG) HEA, which had a consistent uniform elongation of ~21 % and a high yield strength of ~888 MPa. Because of the low stacking fault energy, this good combination of strength and ductility balance was attributed to the excellent ability of CoCrFeMnNi for dislocation storage. Other HEAs systems have also demonstrated exceptional strength and ductility through tuning the grain size [17 - 19].

Although the significant role of cold rolling in strengthening HEAs has been determined, little works on the systematic investigation of the effect of severe cold rolling process on the microstructure and mechanical properties of HEAs has been reported till now [20 - 22]. It is important to remember that during heavy cold rolling without further annealing, considerable strengthening happens at the tradeoff of significantly decreased ductility. The objective of this study is to investigate the effect of heavy cold rolling on the microstructure and mechanical properties of $Fe_{35}Mn_{27}Ni_{28}Co_5Cr_5$ HEA. Additionally, the microstructural evolution provided insight into the strengthening mechanisms in this alloy.

EXPERIMENTAL

High-purity metal powders/pieces (> 99.9 wt %, Alfa Acer Company, Germany) were used to fabricate $Fe_{35}Mn_{27}Ni_{28}Co_5Cr_5$ (in at %) HEA using an induction furnace. Following a 10-hour homogenization process at 900°C, the HEA was air-cooled. The HEAs were then put through rigorous cold rolling procedures using a laboratory rolling mill capable of 20 tons without any lubrication. The thickness reductions of cold rolling were 0 % (as homogenized), 50 %, and 90 %. The roll diameter in this experiment was 180 mm, and the roll peripheral speed was roughly 3 m/min.

A field emission scanning electron microscope (FE-SEM, Jeol JSM7001F, Japan) fitted with an energy dispersive X-ray spectroscopy detector (EDS, Oxford INCA X-max 80, Oxford Instruments, Great Britain) and transmission electron microscopy (TEM, JEM 1200 JEOL, Japan) were carried out to provide the microstructural characterizations. To study the phase constituents by X-ray diffraction (XRD), Cu Kα radiation was used at 40 kV with a tube current of 20 mA in Rigaku Ultima IV X-ray diffractometer (Rigaku, Japan). These measurements were performed using a scanning speed of 2° min^{-1} over a range of 2θ from 5° to 90°.

Vickers microhardness was determined in compliance with the ASTM E384 standard. Tests for Vickers indentation was conducted with loads ranging from 0.1 - 3 N. Electro-discharge machining was used to cut miniature tensile specimens with gauge dimensions of 1.1 mm × 1.0 mm × 0.6 mm according to the rolling (RD), transverse (TD), and normal (ND) directions, respectively, for tensile testing at room temperature. Tensile tests were conducted using a Hounsfield H50KS tensile testing machine (Tinius Olsen Ltd., Redhill, UK) at a nominal strain rate of 10^{-3} s^{-1}.

RESULTS AND DISCUSSION

The XRD patterns of the HEAs in their as-homogenized and cold-rolled states are shown in Fig. 1(a). For every specimen, only a simple FCC phase is found, indicating that the alloys maintain their single FCC structure even in the face of severe plastic deformation. The values of 3.5839, 3.5875, and 3.5894 Å of the lattice parameter (a), which are derived from the XRD patterns (Fig. 1(b)), show that the interplanar distance is gradually decreasing following severe cold rolling. The lattice parameter grows linearly with the cold rolling reduction ratios, ranging from 0 to 90 %. The grains have been refined, as seen by the full width at half maximum (FWHM) of the Bragg diffraction peaks. Also, there is a noticeable variation in the peak intensity ratio I_{200}/I_{111}, which may indicate the formation of texture. This ratio is significantly larger in the cold-rolled states than it is in the as-homogenized case, suggesting that a Brass {011} <211> type texture may occur during the heavy cold-rolling [21, 23, 24].

The back scattered electron SEM (BSE-SEM) images and the corresponding EDS maps of as-homogenized $Fe_{35}Mn_{27}Ni_{28}Co_5Cr_5$ HEA are shown in Fig. 2. The results demonstrate that the initial microstructures consist of a single FCC structure, and

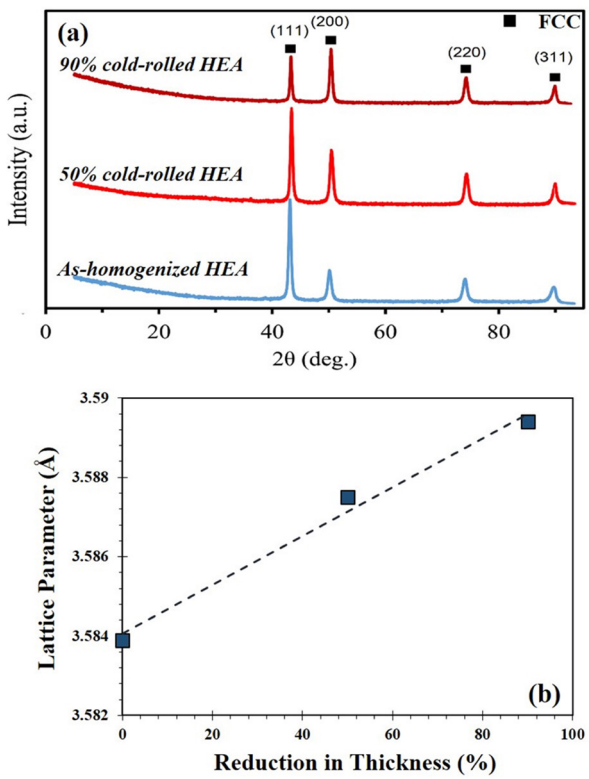

Fig. 1. XRD patterns (a) and lattice parameter versus thickness reduction (b) for $Fe_{35}Mn_{27}Ni_{28}Co_5Cr_5$ HEAs.

a nearly homogenous distribution of the constituent elements is obtained. It should be noted that there is no second phase precipitation in the as-homogenized HEA specimen.

Representative TEM micrographs and the corresponding EDS maps from the RD-ND section of the 50 % and 90 % cold-rolled $Fe_{35}Mn_{27}Ni_{28}Co_5Cr_5$ HEAs are shown in Fig. 3. Regarding Fig. 3(a), grains gradually become elongated in the rolling direction as the cold rolling reduction increases from 0 % to 50 %. On the other hand, dislocations are arranged in various geometries, such as dislocation walls that form sub grain boundaries, tangling of multiple dislocations, and several relatively straight dislocations in one coarse grain [13, 14, 20]. As shown in Fig. 3b, a significant number of pancaked grains and deformation bands are created in the FCC matrix after 90 % cold rolling, which is frequently observed in the severely deformed FCC alloys as a result of localized strain [15, 25].

Metals' plastic behavior is influenced by two main microstructural properties: (i) grain size and (ii) dislocation density. Dislocation density variations during

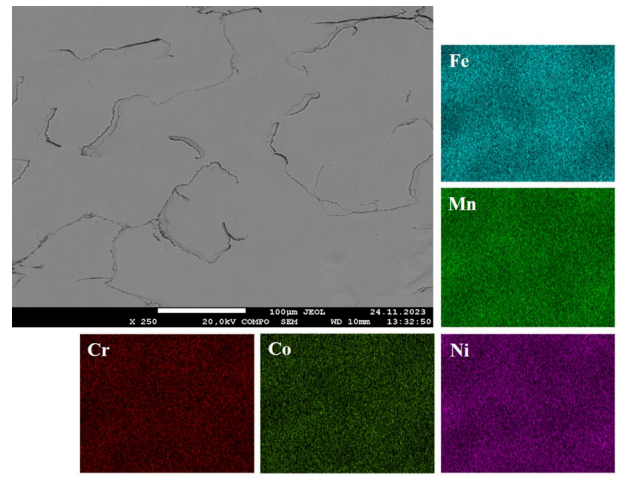

Fig. 2. BSE-SEM images and EDS maps for the as-homogenized $Fe_{35}Mn_{27}Ni_{28}Co_5Cr_5$ HEA.

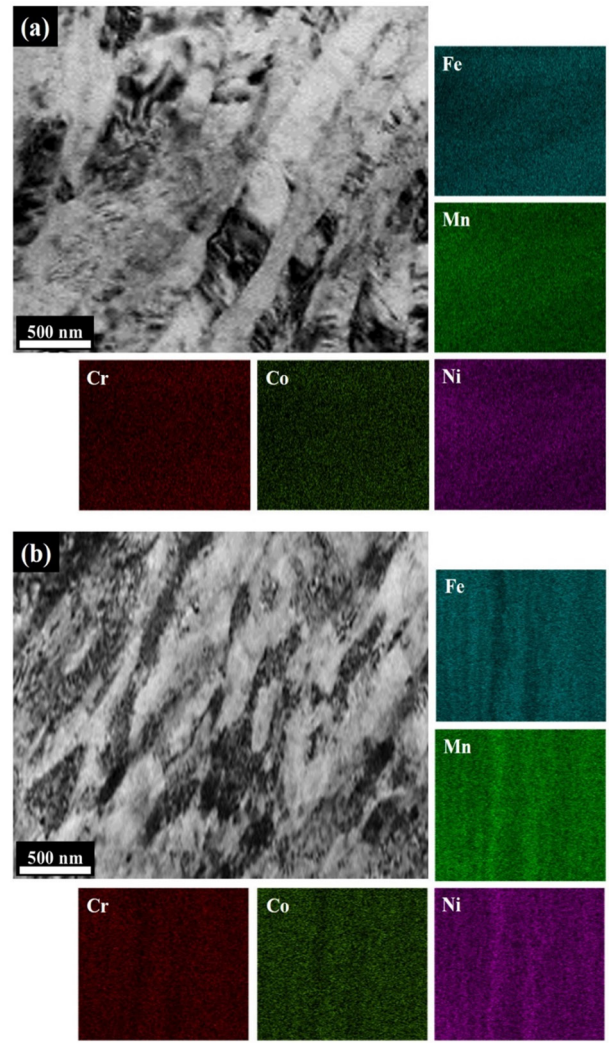

Fig. 3. TEM images and EDS maps for the 50 % (a) and 90 % (b) cold-rolled $Fe_{35}Mn_{27}Ni_{28}Co_5Cr_5$ HEA.

SPD processes are quantitatively investigated using a method based on the use of an indentation size effect (ISE) model [26]. Graca et al. developed a method that uses microhardness values to determine the dislocation density of a metal [27]. They derived a simple expression that connected hardness to indentation depth:

$$\left(\frac{H}{H_0}\right)^2 = 1 + h^*\left(\frac{1}{h}\right) \quad (1)$$

where H_0 is the hardness in the limitation of infinite depth (bulk hardness) and h^* is a characteristic length. By fitting Eq. (1) to the experimental microhardness values, a value of h^* could be obtained. Relating this parameter to the dislocation density has been made feasible by the Nix and Gao model:

$$\rho = \frac{3}{2}\frac{1}{f^3}\frac{\tan^2\theta}{bh^*} \quad (2)$$

where ρ is the density of dislocations stored in the lattice, Θ is the angle between the surface of the sheet and the indenter, b is the burgers vector of the dislocation, and f is a correction factor for the size of the plastic zone. It should be noted that the indentation depth, h, was calculated in [28]:

$$h = \frac{d}{2\sqrt{2}\tan\frac{\theta}{2}} \quad (3)$$

where d is the indentation diameter. In this study $\Theta = 2°$, $f=1.9$, and $b = 0.255$ nm. By introducing these values in Eq. (2), the dislocation density is obtained. Fig. 4 shows the variations of h^* and dislocation density of $Fe_{35}Mn_{27}Ni_{28}Co_5Cr_5$ HEA versus thickness reduction, respectively. It is apparent that the dislocation density increases with increasing cold rolling reduction. The dislocation density increased from 2.28 $\times 10^9$ cm^{-2} (for the as-homogenized specimen) to 7.12 $\times 10^9$ cm^{-2} by 50 % reduction in thickness, registering a 122 % increase. The 50 % reduction in thickness has a remarkable effect on the dislocation density. The value of dislocation density is 8.65 $\times 10^9$ cm^{-2} after 90 % reduction in thickness. Fig. 4 shows that when rolling deformation increased, the dislocation density value first rapidly increased and eventually saturated. Saturation occurs as a result of the materials reaching their steady-state dislocation density, which is determined by the interaction of dislocation generation and annihilation [29, 30].

A summary of the yield strength (YS, calculated with a 0.2 % offset), ultimate tensile strength (UTS), and elongation values of $Fe_{35}Mn_{27}Ni_{28}Co_5Cr_5$ HEA is also shown in Fig. 5. The as-homogenized $Fe_{35}Mn_{27}Ni_{28}Co_5Cr_5$ HEA shows excellent ductility, with an engineering strain at fracture up to 34 %. However, the yield strength is only 225 MPa. By increasing rolling deformation, a remarkable increase in the yield and fracture strength is obtained at the cost of ductility. With a 50 % reduction in thickness, a good balance between YS, UTS, and fracture strain is achieved at 945 MPa, 1150 MPa and 17 %, respectively. At a thickness reduction of 90 %, the tensile strength is 1360 MPa, i.e., 2.8 times that in the as-homogenized state. It can be said that a higher dislocation density leads to higher yield strength. Dislocation hardening provides an important effect on

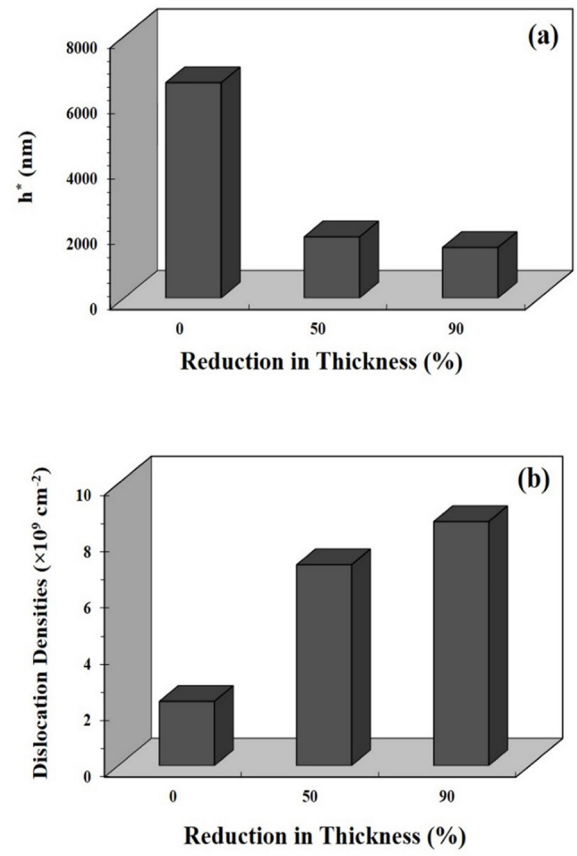

Fig. 4. The h* values (a) calculated by Eq. (1) and dislocation densities (b) for cold-rolled $Fe_{35}Mn_{27}Ni_{28}Co_5Cr_5$ HEA calculated by Eq. (2) based on h* values.

the strength of cold-rolled specimens [7, 8, 20]. The cold-rolled $Fe_{35}Mn_{27}Ni_{28}Co_5Cr_5$ HEA demonstrates a rapidly increased yield and ultimate strength, but that has come at the expense of tensile elongation. A significant number of single FCC phase HEAs exhibit properties comparable to those of austenitic stainless steels or Ni-based alloys, which typically include similar alloying elements, as shown in Fig. 6. Also, in contrast to 2nd generation advanced high strength steels (2nd AHSS), the majority of single FCC phase HEAs have lower ultimate tensile strengths. The results of this study indicate that the severe cold rolling process is a useful technique for enhancing HEAs' mechanical properties.

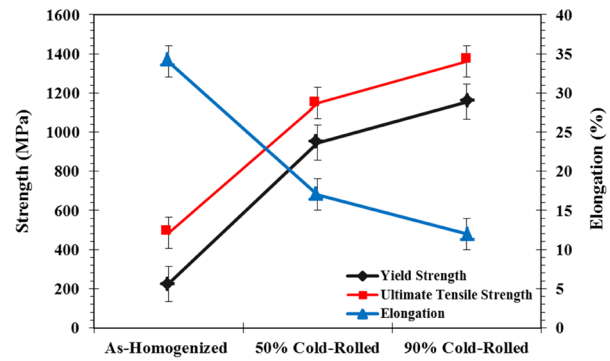

Fig. 5. Yield strength, tensile strength, and uniform elongation plotted of the as-homogenized and cold-rolled HEA specimens.

An estimate of the theoretical strength according to a structure-based strength model can be used to provide important information on the nature of the strengthening mechanisms. The following equation shows a relationship between the microstructure and yield stress for the $Fe_{35}Mn_{27}Ni_{28}Co_5Cr_5$ HEA following a severe cold rolling process by assuming that the yield stress is a simple summation of the strengthening contributions from individual factors that are acting as obstacles for dislocation slip.

$$\sigma = \sigma_0 + \Delta\sigma_{gb} + \Delta\sigma_{dis} \quad (4)$$

where σ_0 is the lattice friction strength assumed as ~ 165 MPa, $\Delta\sigma_{gb}$ and $\Delta\sigma_{dis}$ are the increases in the yield strength caused by grain boundary strengthening and dislocation, respectively. The strengthening of grain boundaries is characterized by the classic Hall-Petch relationship. It is widely recognized that introducing a high-volume percentage of grain boundaries will increase overall strength by impeding dislocation motion caused by grain refinement. $\Delta\sigma_{gb}$ can be calculated by the following equation:

$$\Delta\sigma_{gb} = kd^{-\frac{1}{2}} \quad (5)$$

where k is the strengthening coefficient (226 MPa μm$^{0.5}$ for the $Fe_{35}Mn_{27}Ni_{28}Co_5Cr_5$ HEA) and d is the average

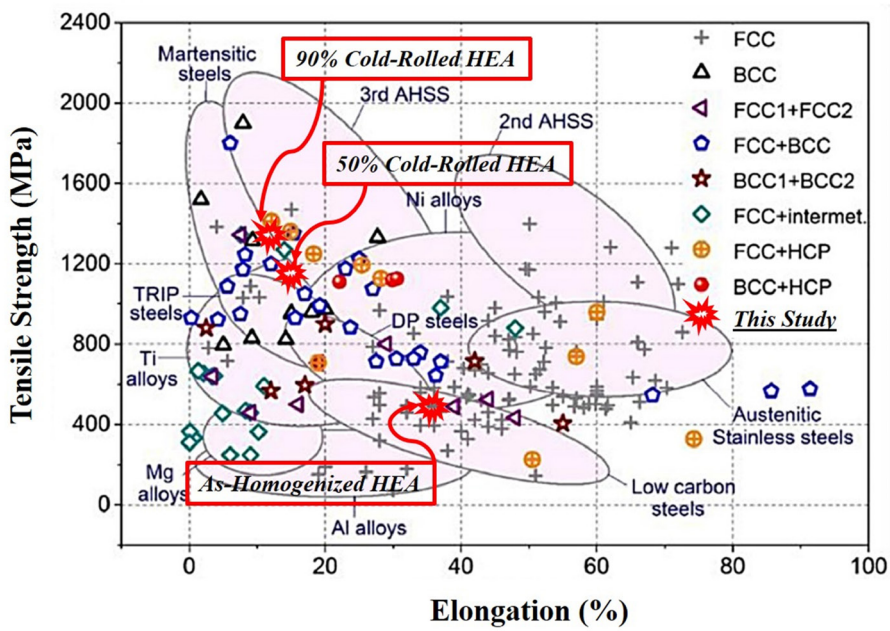

Fig. 6. Schematic of mechanical properties of as-homogenized and cold-rolled $Fe_{35}Mn_{27}Ni_{28}Co_5Cr_5$ HEAs compared with other materials [31].

grain size after 90 % reduction in thickness (185 nm). It then becomes apparent that 625 MPa is the grain refinement contribution to the improved yield strength of UFG $Fe_{35}Mn_{27}Ni_{28}Co_5Cr_5$ HEA.

The dislocation strengthening, $\Delta\sigma_{dis}$, is described by the Bailey-Hirsch relationship through the equation [3]:

$$\Delta\sigma_{dis} = M\alpha Gb\rho^{\frac{1}{2}} \quad (6)$$

where M is the Taylor Factor (3.2), α is a constant (0.33), G is the shear modulus of the $Fe_{35}Mn_{27}Ni_{28}Co_5Cr_5$ HEA (~81 GPa), b is the Burgers vector (0.255 nm), and ρ is the dislocation density after 90% reduction in thickness (8.65×10^9 cm^{-2}). It then becomes apparent that 375 MPa is the dislocation strengthening contribution to the improved yield strength of UFG $Fe_{35}Mn_{27}Ni_{28}Co_5Cr_5$ HEA. The calculated strength obtained using Eq (4) is in good agreement with the experimental value shown in Fig. 5. The most significant strengthening mechanism for severely cold-rolled HEAs specimens, according to an interpretation of the results, is grain boundary strengthening.

CONCLUSIONS

In the present work, severe cold rolling (SCR) was achieved in succession on $Fe_{35}Mn_{27}Ni_{28}Co_5Cr_5$ high-entropy alloy with a series of thickness reductions up to 90 % at ambient temperature. Research was done on the current HEAs' mechanical characteristics and microstructure. The homogenized $Fe_{35}Mn_{27}Ni_{28}Co_5Cr_5$ HEA exhibited a single FCC phase. Also, no phase transformations occurred during cold rolling of the specimens up to a 90 % reduction in thickness. Severe cold rolling resulted in pancaked grains and deformation bands that improved tensile, yield, and hardness properties. 90 % cold-rolled $Fe_{35}Mn_{27}Ni_{28}Co_5Cr_5$ HEA exhibited excellent tensile strength of 1360 MPa, but with a highly decreased elongation of about 12 %. After 90 % reduction in thickness, the dislocation density increased from 2.28×10^9 cm^{-2} (for the as-homogenized specimen) to 8.65×10^9 cm^{-2}, registering a 280 % increase. The cold rolling reduction had a significant effect on the dislocation density. The contribution of grain refinement and dislocation strengthening to the improvement in yield strength was 625 MPa and 375 MPa, respectively.

Acknowledgments

The work was supported financially by the Russian Federation represented by the Ministry of Science and Higher Education of Russian Federation, project number No. 075-15-2023-614.

REFERENCES

1. B. Cantor, I. Chang, P. Knight, A. Vincent, Microstructural development in equiatomic multicomponent alloys, Materials Science and Engineering A, 375, 2004, 213-218.
2. J.W. Yeh, S.K. Chen, S.J. Lin, J.Y. Gan, T.S. Chin, T.T. Shun, C.H. Tsau, S.Y. Chang, Nanostructured high-entropy alloys with multiple principal elements: novel alloy design concepts and outcomes, Advanced engineering materials, 6, 2004, 299-303.
3. W. Li, D. Xie, D. Li, Y. Zhang, Y. Gao, P.K. Liaw, Mechanical behavior of high-entropy alloys, Progress in Materials Science, 118, 2021, 100777.
4. D. Kumar, Recent advances in tribology of high entropy alloys: A critical review, Progress in Materials Science, 136, 2023, 101106.
5. Y. Tang, R. Wang, B. Xiao, Z. Zhang, S. Li, J. Qiao, S. Bai, Y. Zhang, P.K. Liaw, A review on the dynamic-mechanical behaviors of high-entropy alloys, Progress in Materials Science, 135, 2023, 101090.
6. M.J. Yao, K.G. Pradeep, C.C. Tasan, D. Raabe, A novel, single phase, non-equiatomic FeMnNiCoCr high-entropy alloy with exceptional phase stability and tensile ductility, Scripta Materialia, 72-73, 2014, 5-8.
7. H.T. Jeong, W.J. Kim, Microstructures and mechanical properties of the non-equiatomic FeMnNiCoCr high entropy alloy processed by differential speed rolling, Materials Science and Engineering A, 727, 2018, 38-42.
8. Y. Deng, C.C. Tasan, K.G. Pradeep, H. Springer, A. Kostka, D. Raabe, Design of a twinning-induced plasticity high entropy alloy, Acta Materialia, 94, 2015, 124-133.
9. P. Wu, Y. Zhang, L. Han, K. Gan, D. Yan, W. Wu, L. He, Z. Fu, Z. Li, Unexpected sluggish martensitic transformation in a strong and super-ductile high-entropy alloy of ultralow stacking fault energy, Acta Materialia, 261, 2023, 119389.
10. Y. Hu, K. Gan, Y. Zhang, D. Yan, Q. Yang, S. Zhu, Z. Li, Dual-interstitials promoted multiple mechanisms

enhance strength-ductility synergy of an equiatomic high-entropy alloy, Journal of Alloys and Compounds, 968, 2023, 172271.
11. Z. Jiang, W. Chen, C. Chu, Z. Fu, Y. Lu, Y. Ivanisenko, Lamellar-structured low-cost FeMn0.7Ni0.6Cr0.4Al0.3 high entropy alloy with excellent tensile properties, Vacuum, 209, 2023, 111767.
12. J. Čížek, P. Haušild, M. Cieslar, O. Melikhova, T. Vlasák, M. Janeček, R. Král, P. Harcuba, F. Lukáč, J. Zýka, J. Málek, J. Moon, H.S. Kim, Strength enhancement of high entropy alloy HfNbTaTiZr by severe plastic deformation, Journal of Alloys and Compounds, 768, 2018, 924-937.
13. H. Shahmir, P. Asghari-Rad, M.S. Mehranpour, F. Forghani, H.S. Kim, M. Nili-Ahmadabadi, Evidence of FCC to HCP and BCC-martensitic transformations in a CoCrFeNiMn high-entropy alloy by severe plastic deformation, Materials Science and Engineering A, 807, 2021, 140875.
14. Y.L. Bian, Z.D. Feng, N.B. Zhang, Y.X. Li, X.F. Wang, B.B. Zhang, Y. Cai, L. Lu, S. Chen, X.H. Yao, S.N. Luo, Ultrafast severe plastic deformation in high-entropy alloy Al0.1CoCrFeNi via dynamic equal channel angular pressing, Materials Science and Engineering A, 847, 2022, 143221.
15. J. Xu, Q. Liu, Y.F. Xu, S.H. Guo, C. Li, N.B. Zhang, Y. Cai, X.Y. Liu, L. Lu, S.N. Luo, Taylor impact of high-entropy alloy Al0.1CoCrFeNi: Dynamic severe plastic deformation and bulk gradient structure, Journal of Alloys and Compounds, 936, 2023, 168261.
16. B. Schuh, F. Mendez-Martin, B. Völker, E.P. George, H. Clemens, R. Pippan, A. Hohenwarter, Mechanical properties, microstructure and thermal stability of a nanocrystalline CoCrFeMnNi high-entropy alloy after severe plastic deformation, Acta Materialia, 96, 2015, 258-268.
17. Z.Y. You, Z.Y. Tang, B. Wang, H.W. Zhang, P. Li, L. Zhao, F.B. Chu, H. Ding, Microstructural evolution and deformation behavior of an interstitial TRIP high-entropy alloy under dynamic loading, Materials Science and Engineering A, 891, 2024, 145931.
18. Y. Li, Z. Yang, P. Wang, H. Duan, W. Yang, Z. Ma, C. Wu, J. Li, The nanocrystalline and high density dislocation-Enabled ultrahigh strength and ductility of Al0.4Co0.5V0.2FeNi high entropy alloy, Materials & Design, 236, 2023, 112493.
19. R.R. Eleti, B. Allen, B. Martin, D. Sathiaraj, S.S.S. Kumar, Grain boundary sliding with diffusional accommodation enable dynamic recrystallization during hot deformation of coarse-grained body-centered cubic HfNbTaTiZr high-entropy alloys, Scripta Materialia, 238, 2024, 115778.
20. Y. Wang, J. Chen, R. Ding, W. Wang, J. He, X. Zhou, Effect of cold rolling on microstructure and mechanical property of a novel (Fe50Mn30Co10Cr10)97C2Mo1 high entropy alloy, Journal of Materials Research and Technology, 27, 2023, 6065-6075.
21. Z. Li, L. Fu, J. Peng, H. Zheng, A. Shan, Effect of annealing on microstructure and mechanical properties of an ultrafine-structured Al-containing FeCoCrNiMn high-entropy alloy produced by severe cold rolling, Materials Science and Engineering A, 786, 2020, 139446.
22. M. Naseri, A.O. Moghaddam, N. Shaburova, D. Gholami, A. Pellenen, E. Trofimov, Ultrafine lamellar microstructures for enhancing strength-ductility synergy in high-entropy alloys via severe cold rolling process, Journal of Alloys and Compounds, 965, 2023, 171385.
23. T. Sun, W. Song, F. Shan, K. Song, K. Zhang, C. Peng, H. Sun, L. Hu, Phase formation, texture evolutions, and mechanical behaviors of Al0.5CoCr0.8FeNi2.5V0.2 high-entropy alloys upon cold rolling, Progress in Natural Science: Materials International, 32, 2022, 196-205.
24. A. Shabani, M.R. Toroghinejad, A. Shafyei, P. Cavaliere, Effect of cold-rolling on microstructure, texture and mechanical properties of an equiatomic FeCrCuMnNi high entropy alloy, Materialia, 1, 2018, 175-184.
25. G.D. Sathiaraj, P.P. Bhattacharjee, Effect of cold-rolling strain on the evolution of annealing texture of equiatomic CoCrFeMnNi high entropy alloy, Materials Characterization, 109, 2015, 189-197.
26. W.D. Nix, H. Gao, Indentation size effects in crystalline materials: a law for strain gradient plasticity, Journal of the Mechanics and Physics of Solids, 46, 1998, 411-425.
27. S. Graça, R. Colaço, P. Carvalho, R. Vilar, Determination of dislocation density from hardness measurements in metals, Materials Letters, 62, 2008, 3812-3814.
28. W.D. Callister, D.G. Rethwisch, Materials Science and Engineering: An Introduction, 8th Edition, London, Wiley, 2009.

29. M. Naseri, D. Gholami, O. Imantalab, F.R. Attarzadeh, A. Fattah-alhosseini, Effect of grain refinement on mechanical and electrochemical properties of severely deformed pure copper through equal channel angular pressing, Materials Research Express, 5, 2018, 076504.
30. A. Keyvani, M. Naseri, O. Imantalab, D. Gholami, K. Babaei, A. Fattah-alhosseini, Microstructural characterization and electrochemical behavior of nano/ultrafine grained pure copper through constrained groove pressing (CGP), Journal of Materials Research and Technology, 11, 2021, 1918-1931.
31. E.P. George, W.A. Curtin, C.C. Tasan, High entropy alloys: A focused review of mechanical properties and deformation mechanisms, Acta Materialia, 188, 2020, 435-474.